

Modeliranje sestavov kovine in elastomerov z uporabo postopka končnih elementov

Modelling Metal-Elastomer Composite Structures Using a Finite-Element-Method Approach

Sergio E. Floody¹ - Jorge P. Arenas² - José J. de Espíndola³

(¹Technical University of Chile; ²Austral University of Chile; ³Federal University of Santa Caterina, Brasil)

Sestavi kovine in elastomerov so pomembno orodje za zmanjšanje mehanskih nihanj. Pri upogibu nihajoči sestav lahko dušimo z dodatkom primerne plasti dušilnega materiala, na primer elastomera, kjer je plast izpostavljena ciklični deformaciji in na ta način tudi izgubi energije. Vendar pa prisotnost elastomera pomeni, da je sestav odvisen od frekvence, zaradi tega težko natančno napovedujemo, saj je težko izračunati rešitev ustreznega problema lastnih vrednosti. V prispevku je predstavljena metodologija za modeliranje sestavov kovine in elastomerov z uporabo metode končnih elementov. V nadaljevanju je obravnavana računrska metoda določitve približne rešitve frekvenčno odvisnega problema lastnih vrednosti. Številčne rezultate vztrajnosti smo primerjali z rezultati preizkusa običajnega "sendvič" sestava grede. Metodo smo razširili na model in tako optimirali Stockbridgove dušilnike, ki so uporabljani za dušenje zračnih nihanj dejanskega električnega daljnovoda. Namesto uglasitve dušilnika na neko določeno frekvenco, smo z uporabo genskih algoritmov določili ciljno funkcijo in optimirali fizikalne izmere dušilnika. S takim postopkom smo analizirali celoten problem brez uporabe modalnega pristopa napetost-energija, kar pomeni, da ta tako modeliranje zadosti načelu vzorčnosti. Metoda je uporabna kot orodje za načrtovanje in modeliranje sestavov kovine in elastomerov.

© 2007 Strojniški vestnik. Vse pravice pridržane.

(Ključne besede: kompoziti kovine - elastomeri, modeliranje strukture, metode končnih elementov, dušilniki vibracij)

Metal-elastomer composite structures are an important tool for the reduction of mechanical vibrations. A structure that vibrates in flexure can be damped by the appropriate addition of a layer of damping material, for example, an elastomer, where the layer undergoes cyclic strain and thereby dissipates energy. However, the presence of the elastomer means that the structure is frequency dependent, which is a difficult case for obtaining accurate predictions since the solution of the corresponding eigenvalue problem is hard to compute. In this paper a methodology for modelling metal-elastomer composite structures using a finite-element approach is presented. In addition, a calculation scheme to approximate the solution of the frequency-dependent eigenvalue problem is discussed. The numerical results for the inertness were compared with the experimental results for a classic composite sandwich beam. The method is extended to model and optimise Stockbridge absorbers used to suppress the aeolian vibrations of an actual electrical transmission line. Instead of tuning the absorber to some particular frequency, an objective function is defined and the physical dimensions of the absorber are optimised by means of a genetic algorithm. In this approach, the complete problem is analysed without using the modal strain-energy approach, implying that this modelling satisfies the causality principle. The method appears to be useful as a tool for designing and modelling metal-elastomer composite structures.

© 2007 Journal of Mechanical Engineering. All rights reserved.

(Keywords: metal elastomer composite, structure modelling, finite element methods, Stockbridge dampers)

0 INTRODUCTION

Metal-elastomer composite structures are an important tool for the reduction of mechanical vibra-

tions. A structure that vibrates in flexure can be damped by the appropriate addition of a layer of damping material. As the whole system vibrates, the layer undergoes cyclic strain and thereby dissipates

energy. Since the first successful modelling of a metal-elastomer composite presented by Ross et al. [1], considerable attention has been paid to the prediction of the dynamic behaviour of such structures. For many years, the finite element method has been used for modelling structures, and several of its applications have been shown to be quite accurate. Soni [2] has presented a finite element analysis of viscoelastically damped sandwich beams, which uses a combination of shell elements and three dimensional solids for the viscoelastic part. Another approach is to use shell elements with spring elements to model the elastomer [3]. This methodology has been shown to increase the speed of the calculations of the stiffness and mass matrices. Lumsdaine et al. [4] have reported a method using multi-layer elements, which has been proven to be very accurate. Although the modelling using three dimensional solid elements is the most complete alternative to solve this kind of problem, sometimes the computational cost of formulating and solving the equations can become prohibitive.

The viscoelastic materials of greatest practical interest for damping applications are plastics and elastomers. An elastomer is a soft substance that exhibits thermo-viscoelastic behaviour. Viscoelastic materials possess both elastic and viscous properties. For a purely elastic material, all the energy stored in a sample during loading is returned when the load is removed. Furthermore, the displacement of the sample responds immediately, and in-phase, to the cyclic load. Conversely, for a purely viscous material, no energy is returned after the load is removed. The input stress is lost to pure damping as the vibration energy is transferred to internal heat energy. All the materials that do not fall into one of the above extreme classifications are called viscoelastic materials. Some of the energy stored in a viscoelastic system is recovered upon removal of the load, and the remaining energy is dissipated by the material in the form of heat.

In a metal-viscoelastic-metal structure, the bending of the composite produces not only bending and extensional strains in all three layers, but also shears, primarily of the middle (viscoelastic) layer. The shear-strain energy storage tends to dominate the damping action of the constrained viscoelastic layers. Many practical applications operate on the principle of constrained layer damping. The shear forces in the constrained viscoelastic layer cause the energy of the vibration to be converted into heat.

Undamped metal structures normally have a very low loss factor, typically in the range 0.001 to 0.01. Using a viscoelastic layer can increase this loss factor. This means that the amplitude of the resonant vibration when the structure is subjected to structure-borne sound or vibration will be much lower than for an undamped structure. A reduced amplitude of vibration means less radiation of sound, and also a reduced risk of fatigue failure [5].

A characteristic of viscoelastic materials is that their Young's modulus is a complex quantity, having both a real and imaginary component. Furthermore, this complex modulus varies as a function of many parameters, the most important of which are the frequency and temperature of a given application. Consequently, this results in a corresponding eigenvalue problem in which the stiffness matrix depends on both the frequency and the temperature. The moduli typically take on relatively high values at low temperatures and/or high frequencies but take on comparatively small values at high temperatures and/or low frequencies. It is therefore necessary to establish an accurate understanding of the influence of these parameters in order to design effective damping treatments.

In general, the vibration analysis of a system that is frequency independent can be accurately achieved by classical techniques. It is much more difficult to obtain accurate predictions when the equations of motion are frequency dependent. This is because the solution of the corresponding eigenvalue problem is difficult to compute. Methods based on the modal strain energy have been used to approximate the solution of the problem [2]. However, they are not accurate when the frequency and temperature ranges are increased, and when they include the *transition region*, where the variations of the dissipation and the stiffness of the viscoelastic material are quite pronounced. The greatest loss factors occur in the transition region at intermediate frequencies and temperatures. On the other hand, some of the assumptions used by these methods do not fit the principle of causality for physical systems [6].

The final aim of this paper is to present a methodology to model metal-elastomer composite structures by using a finite-element approach. The method was experimentally tested for a classic composite sandwich beam. Then, an application to model and optimise a Stockbridge absorber used to suppress the aeolian vibrations of an electrical transmission line is presented.

1 THEORY

The theory of finite element methods has been clearly presented by several authors ([7] to [9]), so it will not be repeated here. However, a method to avoid inverting matrices of a large size will be discussed in this section, since it is quite useful to speed up the numerical solution.

As a result of the modelling using finite elements of a metal-elastomer structure, a frequency-dependent equation of motion is obtained. The equations of motion as a function of frequency for a forced multi-degree-of-freedom system and its associated eigenvalue problem can be written as:

$$[-\Omega^2 \mathbf{M} + \mathbf{K}(\Omega, T)] \mathbf{q}(\Omega, T) = \mathbf{f}(\Omega) \quad (1),$$

and

$$\mathbf{K}(\Omega, T) \boldsymbol{\varphi}(\Omega, T) = \sigma(\Omega, T) \mathbf{M} \boldsymbol{\varphi}(\Omega, T) \quad (2),$$

where Ω is the angular frequency, T is a fixed temperature, \mathbf{M} is the mass matrix, $\mathbf{K}(\Omega, T)$ is the stiffness matrix, $\mathbf{q}(\Omega, T)$ is the modal displacement vector, $\mathbf{f}(\Omega)$ is the vector of external forces, $\boldsymbol{\varphi}(\Omega, T)$ is an eigenvector associated with the vibration modes, and $\sigma(\Omega, T)$ is an eigenvalue associated with a natural frequency.

In general, a direct solution of Eq. (2) will involve an expensive and inefficient method because of the large size of the matrices. Therefore, a proposed algorithm to simplify the task can be summarized as:

1) Solve the eigenvalue problem of order n for an arbitrary fixed frequency Ω_0 , and for a value of temperature T , given by:

$$\mathbf{K}(\Omega_0, T) \boldsymbol{\varphi}(\Omega_0, T) = \sigma(\Omega_0, T) \mathbf{M} \boldsymbol{\varphi}(\Omega_0, T) \quad (3).$$

Now, the modal matrix Φ_0 has the following properties:

$$\Phi_0^T \mathbf{M} \Phi_0 = \mathbf{I}_n \quad (4),$$

and

$$\Phi_0^T \mathbf{K}(\Omega_0, T) \Phi_0 = \boldsymbol{\Sigma}_0 \quad (5),$$

where the superscript T denotes the transpose, \mathbf{I}_n is the $n \times n$ identity matrix, and $\boldsymbol{\Sigma}_0 = \text{diag}(\sigma_0)$ is a diagonal matrix of eigenvalues.

2) Let $\hat{\Phi}_0$ be an $n \times \hat{n}$ truncated matrix of the \hat{n} eigenvectors associated with the minor eigenvalues ($\hat{n} < n$). For a frequency $\Omega \neq \Omega_0$, the following product is calculated:

$$\hat{\Phi}_0^T \mathbf{K}(\Omega, T) \hat{\Phi}_0 = \boldsymbol{\Sigma}(\Omega, T) \quad (6),$$

where the matrix $\boldsymbol{\Sigma}(\Omega, T)$ is not necessarily diagonal, but it is an $\hat{n} \times \hat{n}$ matrix. Then, the new eigenvalue problem can be stated as:

$$\boldsymbol{\Sigma}(\Omega, T) \boldsymbol{\psi}(\Omega, T) = \lambda(\Omega, T) \boldsymbol{\psi}(\Omega, T) \quad (7),$$

$$\boldsymbol{\Psi}^T(\Omega, T) \boldsymbol{\Psi}(\Omega, T) = \mathbf{I}_{\hat{n}} \quad (8),$$

and

$$\boldsymbol{\Psi}^T(\Omega, T) \boldsymbol{\Sigma}(\Omega, T) \boldsymbol{\Psi}(\Omega, T) = \boldsymbol{\Lambda}(\Omega, T) \quad (9),$$

where $\lambda(\Omega, T)$ and $\boldsymbol{\psi}(\Omega, T)$ are the eigenvalue and eigenvector, respectively, $\mathbf{I}_{\hat{n}}$ is the $\hat{n} \times \hat{n}$ identity matrix, $\boldsymbol{\Psi}(\Omega, T)$ is a modal matrix, and $\boldsymbol{\Lambda}(\Omega, T) = \text{tr}(\lambda_i(\Omega, T))$ is a trace matrix of eigenvalues. The new eigenvalue problem is still frequency dependent, but it is a problem of smaller size and consequently requires less computation time.

3) Consider the following transformation of coordinates:

$$\mathbf{q}(\Omega, T) = \hat{\Phi}_0 \mathbf{r}(\Omega, T) \quad (10),$$

and

$$\mathbf{r}(\Omega, T) = \boldsymbol{\Psi}(\Omega, T) \mathbf{p}(\Omega, T) \quad (11).$$

Substituting Eq. (10) and (11) into Eq. (1), and pre-multiplying by $[\hat{\Phi}_0 \boldsymbol{\Psi}(\Omega, T)]^T$ gives

$$[-\Omega^2 \mathbf{I}_{\hat{n}} + \boldsymbol{\Lambda}(\Omega, T)] \mathbf{p}(\Omega, T) = [\hat{\Phi}_0 \boldsymbol{\Psi}(\Omega, T)]^T \mathbf{f}(\Omega) \quad (12).$$

Thus, the nodal displacement vector is given by:

$$\mathbf{q}(\Omega, T) = \hat{\Phi}_0 \boldsymbol{\Psi}(\Omega, T) [-\Omega^2 \mathbf{I}_{\hat{n}} + \boldsymbol{\Lambda}(\Omega, T)]^{-1} [\hat{\Phi}_0 \boldsymbol{\Psi}(\Omega, T)]^T \mathbf{f}(\Omega) \quad (13).$$

Therefore, the receptance matrix is obtained from Eq. (13) as:

$$\boldsymbol{\alpha}(\Omega, T) = \hat{\Phi}_0 \boldsymbol{\Psi}(\Omega, T) [-\Omega^2 \mathbf{I}_{\hat{n}} + \boldsymbol{\Lambda}(\Omega, T)]^{-1} [\hat{\Phi}_0 \boldsymbol{\Psi}(\Omega, T)]^T \quad (14).$$

Defining the matrix product $\mathbf{S}(\Omega, T) = \hat{\Phi}_0 \boldsymbol{\Psi}(\Omega, T)$, Eq. (14) can be re-written as:

$$\boldsymbol{\alpha}(\Omega, T) = \mathbf{S}(\Omega, T) [-\Omega^2 \mathbf{I}_{\hat{n}} + \boldsymbol{\Lambda}(\Omega, T)]^{-1} \mathbf{S}^T(\Omega, T) \quad (15),$$

where $\boldsymbol{\Sigma}(\Omega, T) = \boldsymbol{\Lambda}(\Omega, T)$ for all Ω and T . Consequently, the inertness matrix is:

$$-\Omega^2 \boldsymbol{\alpha}(\Omega, T) = -\Omega^2 \mathbf{S}(\Omega, T) [-\Omega^2 \mathbf{I}_{\hat{n}} + \boldsymbol{\Lambda}(\Omega, T)]^{-1} \mathbf{S}^T(\Omega, T) \quad (16).$$

Then, the corresponding elements of the receptance matrix $\alpha(\Omega, T)$ are:

$$\alpha_{ij}(\Omega, T) = \sum_{k=1}^{\hat{n}} \frac{s_{ik}(\Omega, T) s_{jk}(\Omega, T)}{\lambda_k(\Omega, T) - \Omega^2} \quad (17),$$

where s is an element of the matrix $\mathbf{S}(\Omega, T)$, and $\lambda_k(\Omega, T) \cong \sigma_k(\Omega, T)$.

Therefore, the $\hat{n} \times \hat{n}$ matrix $\Sigma(\Omega, T)$ can be assumed to be a projection of the stiffness matrix into an approximated subspace of the space formed by the real eigenvectors. So the quality of the approximation depends on the subspace, or $span\{\varphi_{01}, \dots, \varphi_{0h}\}$.

An important detail for stating the problem of Eq. (1) is the construction of the stiffness matrix $\mathbf{K}(\Omega, T)$. This construction can be done by using the finite element method for each frequency. If $\mathbf{K}(\Omega, T)$ is a matrix of large size, it can be computed for several frequencies by means of a Taylor series expansion in the neighbourhood of a transition frequency Ω_t as:

$$\mathbf{K}(\Omega, T) = \sum_{m=0}^M \frac{\mathbf{K}^{(m)}(\Omega_t, T)}{m!} (\Omega - \Omega_t)^m \quad (18),$$

where

$$\mathbf{K}^{(m)}(\Omega, T) = \frac{d^m \mathbf{K}(\Omega, T)}{d\Omega^m} \quad (19).$$

It is then relatively easy to compute the derivatives $\mathbf{K}^{(m)}(\Omega, T)$ since only the elementary stiffness matrices of the viscoelastic part are frequency dependent, while the derivatives of the stiffness matrices of the metal part are not. The use of $M=3$ for the series expansions shows that the results are quite exact for a narrow frequency band in the neighbourhood of a transition frequency.

2 RESULTS

2.1 Composite Sandwich-Beam

The first example of the application of the theory presented above is a simple clamped-free composite sandwich beam. This kind of structure is commonly used as a study object. The sandwich beam is made of two metal layers of steel 1020 and a viscoelastic core made of DYAD 601 material (Soundcoat Co.). The viscoelastic core was attached in between the metal layers by means of an epoxic-

structural adhesive. The properties of this viscoelastic material were presented in reference [10]. The beam was 211.85 mm long and 11.97 mm wide. The thickness of each metal layer was 2.14 mm and the thickness of the viscoelastic core was 0.5 mm. All the dimensions of the sandwich composite beam are in accordance to the requirements of the ASTM E 756-98 standard [11].

The composite sandwich beam was divided into 114 two-dimensional Lagrangian solid elements on a plane state of stress. Along the beam 19 elements were selected at equal intervals and each layer was divided into two elements, resulting in a total of 507 nodes, having two degrees of freedom at each node, so $n=1014$ for this application. The above parameters of the structure were selected because they assured the determination of the first four modes and the modal damping produced by the shear deformation of the core.

An experimental set-up was devised to perform a dynamic test to measure the frequency response of the beam. The beam was excited using a magnetic actuator (B&K MM0002). The signal fed to the actuator was a chirp excitation between 0 to 1600 Hz, i.e., a sine wave of linearly increasing frequency, and amplified by a power amplifier (B&K 2706). The response of the beam was measured by a small accelerometer (B&K 4375). The signals were analysed using a two-channel FFT analyser (HP 3567A). The experimental set-up was placed inside a chamber in which the temperature could be controlled in the range between -30 and 60°C . The precision of the chamber was $\pm 1^\circ\text{C}$. The excitation was applied at 59.64 mm from the clamped edge, which corresponds to node 143 in the finite element mesh, and the response was measured at 37.95 mm from the clamped edge, which corresponds to node 91 in the finite element mesh (see Fig. 1).

Computation of the inertness was developed for different temperatures ranging between -30 and 60°C , and they were compared with the results obtained experimentally. In the computation $\hat{n}=50$ was used for the theory presented in Section 1. Figures 2

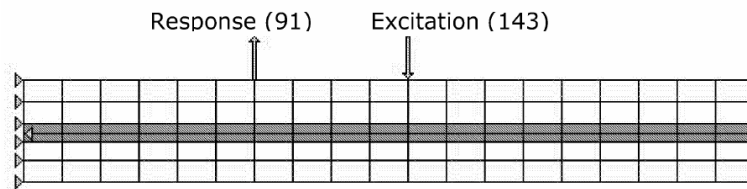


Fig. 1. Finite element model for the clamped-free sandwich composite beam

to 4 show the results of the inertness for three different temperatures.

From the results the effect on the natural frequencies caused by the increase in stiffness of the elastomer in the transition region ($-10^{\circ}\text{C} < T < 20^{\circ}\text{C}$) can be seen. In fact, in this region, the value of the fourth natural frequency increased so much that it fell out of the frequency range of the measurement. There is reasonable agreement between the numerical and experimental results for the inertness frequency responses presented in Figures 2 to 4, although it is observed that the numerical results seem to underpredict the natural frequencies when compared with those obtained from the experimental set-up. The differences are on average about 6%. Nevertheless, the differences between the numerical and experimental approaches can be due to imperfections in the experimental fixture, the small size of the structure under test, the contribution of the off-resonant modes, and the measurement uncertainty produced by the environment inside the chamber. The effect of the chamber should be more pronounced in the transition region, where small variations of temperature will cause large variations on the elastic properties of the elastomer. The value of the humidity inside the chamber was not accurately controlled during the experiment. This fact was reflected as noise in the measured inertness frequency-response curves, as seen in Figures 2 to 4.

2.2 Stockbridge Dynamic Vibration Absorber

In this section the theory will be applied to a more complicated case, i.e., a Stockbridge dynamic

vibration absorber. The vibration absorber will be viscoelastically modified in order to increase the dissipation of vibrational energy.

A dynamic vibration absorber, also called a vibration neutralizer, is a device or structure (secondary system) that is attached to another device (primary system) to reduce vibration levels. It acts on the primary system by applying reaction forces and dissipating vibration energy. Vortex-induced or aeolian vibrations of overhead electrical transmission lines, also referred to as conductors, are very common and can lead to fatigue damage. These vibrations are usually caused by winds ranging in velocity from 1 to 7 m/s and can occur at frequencies from 3 to 150 Hz with peak-to-peak displacement amplitudes of up to one conductor diameter. In conventional transmission line systems, one or more Stockbridge absorbers may be attached to a conductor in an effort to suppress the aeolian vibrations ([12] and [13]).

The classic theory introduced by den Hartog [14] for a viscous vibration absorber, called MCK, and their extensions to a viscoelastic absorber, presented by Snowdon [15], are difficult to apply. This is because for complex mechanical systems many modes can contribute to the total response of the primary system. Interesting methods to optimise dynamic vibration absorbers have been presented by Brennan and co-workers ([16] to [19]). Kidner and Brennan [17] used a multi-degree-of-freedom beam neutralizer with piezoceramic patches as active elements, and they analysed the improvement on the performance of the absorber considering the rigid

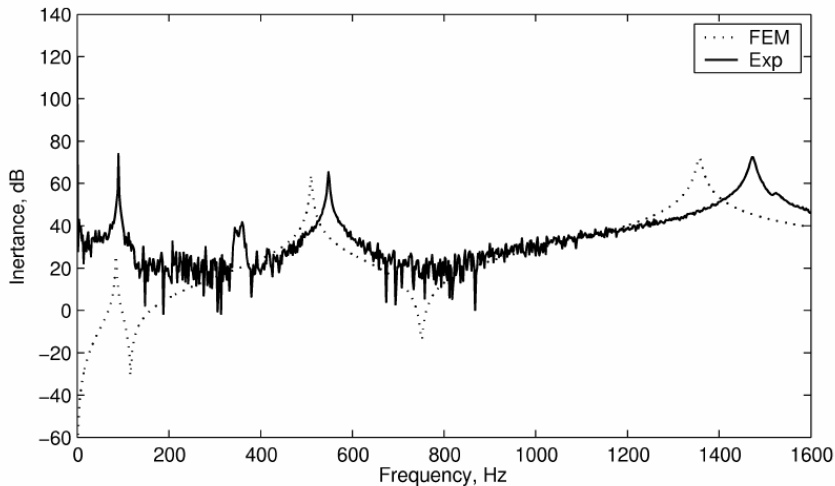


Fig. 2. Comparison of the experimental and numerical results for the inertance frequency response of the beam at -30°C

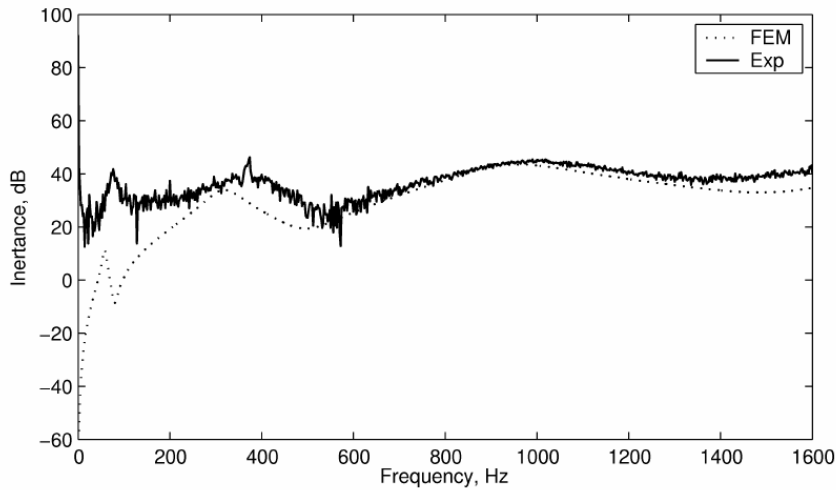


Fig. 3. Comparison of the experimental and numerical results for the inertness frequency response of the beam at 10 °C

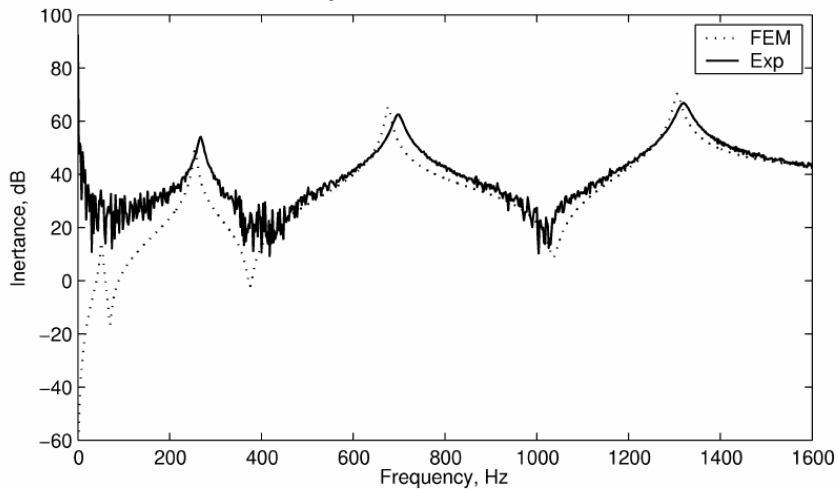


Fig. 4. Comparison of the experimental and numerical results for the inertness frequency response of the beam at 60 °C

body mode and the first mode of the beam in their analysis. Brennan and Dayou [18] used an equivalent damper to represent the dynamic stiffness of the absorber assuming a very low damping. Then, they were able to model the problem without adding degrees of freedom, but by using all the modes of the primary structure. More recently, an experimental verification of the optimum tuning method has been presented [19]. An interesting finding is that the absorber can be as effective as active control in reducing the global vibration of the structure. On the other hand, Espindola and Silva [20] introduced the concept of generalized equivalent quantities. The basic idea of their technique is to transform the mechanical impedance of the absorber's coupling point to the primary system, into generalized

quantities of mass and damping that are frequency dependent. Using the generalized quantities it is possible to formulate the compound equations of motion simply in terms of the generalized coordinates of the primary system. After the equations are written in the principal coordinates, and retaining those that correspond to the frequency band of interest (where the problem of high response residua), the computations are made in a modal subspace, which includes just a minimum number of equations.

2.3 Finite-Element Model for the Secondary System

In simple terms a Stockbridge absorber is composed of a mass at the centre, two attached

sandwich (metal-elastomer-metal) beams, and two attached tuning masses, as shown in Figure 5. The mass at the centre is attached to the primary system. The finite element method is used to model the absorber's behaviour. The corresponding eigenvalue problem, which is frequency dependent, can be solved using the technique presented in Section 1. The finite element model of the absorber is shown in Figure 5. Now, for a fixed temperature the equations of motion for the secondary system are:

$$\mathbf{M}\ddot{\mathbf{u}} + \mathbf{K}(\Omega)\mathbf{u} = \mathbf{f}(t) \quad (20).$$

After modification of the order of rows and columns in order to appropriately place the control node, as shown in Figure 5, we can define:

$$\mathbf{u} = [q_1, q_2, \dots, q_{n-1}, y]^T = [\mathbf{q}, y]^T \quad (21),$$

$$\mathbf{f}(t) = [0, 0, \dots, 0, f(t)]^T = [\mathbf{0}, f(t)]^T \quad (22),$$

and then Eq. (20) can be written in partitioned matrix form as:

$$\begin{bmatrix} \mathbf{M}_1 & \mathbf{M}_2 \\ \mathbf{M}_3 & \mathbf{M}_4 \end{bmatrix} \begin{bmatrix} \ddot{\mathbf{q}} \\ \ddot{y} \end{bmatrix} + \begin{bmatrix} \mathbf{K}_1(\Omega) & \mathbf{K}_2(\Omega) \\ \mathbf{K}_3(\Omega) & \mathbf{K}_4(\Omega) \end{bmatrix} \begin{bmatrix} \mathbf{q} \\ y \end{bmatrix} = \begin{bmatrix} \mathbf{0} \\ f(t) \end{bmatrix} \quad (23),$$

where \mathbf{M}_1 is an $n-1 \times n-1$ mass submatrix, \mathbf{M}_2 is an $n-1 \times 1$ mass submatrix, \mathbf{M}_3 is a $1 \times n-1$ mass submatrix, \mathbf{M}_4 is a 1×1 mass submatrix, $\mathbf{K}_1(\Omega)$ is an $n-1 \times n-1$ stiffness submatrix, $\mathbf{K}_2(\Omega)$ is an $n-1 \times 1$ stiffness submatrix, $\mathbf{K}_3(\Omega)$ is a $1 \times n-1$ stiffness submatrix,

$\mathbf{K}_4(\Omega)$ is a 1×1 stiffness submatrix, \mathbf{u} is the total displacement vector, \mathbf{q} is the displacement vector without considering the control node, y is the displacement of the control node, and $f(t)$ is the force applied to the absorber by the primary system. Now, in the frequency domain, Eq. (23) can be expressed as the system of equations:

$$\begin{aligned} [-\Omega^2 \mathbf{M}_1 + \mathbf{K}_1(\Omega)]\mathbf{Q}(\Omega) + [-\Omega^2 \mathbf{M}_2 + \mathbf{K}_2(\Omega)]\mathbf{Y}(\Omega) &= \mathbf{0} \\ [-\Omega^2 \mathbf{M}_3 + \mathbf{K}_3(\Omega)]\mathbf{Q}(\Omega) + [-\Omega^2 \mathbf{M}_4 + \mathbf{K}_4(\Omega)]\mathbf{Y}(\Omega) &= \mathbf{F}(\Omega) \end{aligned} \quad (24).$$

After solving Eq. (24), we obtain the dynamic stiffness of the system as:

$$K(\Omega) = \frac{F(\Omega)}{Y(\Omega)} = \mathbf{X}_4(\Omega) - \mathbf{X}_3(\Omega)\mathbf{X}_1^{-1}(\Omega)\mathbf{X}_2(\Omega) \quad (25),$$

where:

$$\mathbf{X}_i(\Omega) = -\Omega^2 \mathbf{M}_i + \mathbf{K}_i(\Omega), \text{ for } i=1, \dots, 4 \quad (26).$$

Now, the inverse of \mathbf{X}_1 can be computed approximately by using Eq. (15), as:

$$\mathbf{X}_1^{-1}(\Omega) = [-\Omega^2 \mathbf{M}_1 + \mathbf{K}_1(\Omega)]^{-1} \cong \mathbf{S}(\Omega) [-\Omega^2 \mathbf{I}_n + \mathbf{\Lambda}(\Omega)]^{-1} \mathbf{S}^T(\Omega) \quad (27).$$

From the dynamic stiffness we can obtain the dynamic impedance

$$Z(\Omega) = \frac{K(\Omega)}{j\Omega} \quad (28),$$

where $j = \sqrt{-1}$, and the apparent mass

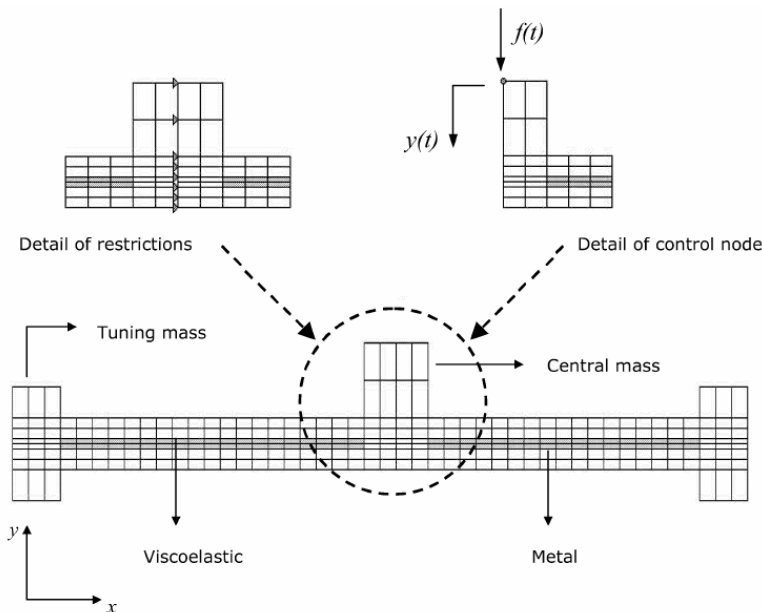


Fig. 5. Finite element model for the Stockbridge dynamic vibration absorber

$$M(\Omega) = \frac{K(\Omega)}{-\Omega^2} \quad (29).$$

Consequently, the equivalent damping and equivalent mass are

$$c_{eq}(\Omega) = \Re\{Z(\Omega)\} \quad (30),$$

and

$$m_{eq}(\Omega) = \Re\{M(\Omega)\} \quad (31),$$

respectively.

Then, the model of the absorber is replaced by an equivalent mechanical system composed of an equivalent mass connected to the primary system and an equivalent damper connected to the ground, where both are frequency dependent. In this way there are new physical degrees of freedom in the mechanical system, but there are no new degrees of freedom in the model. This formulation is equivalent to the simple model of a Stockbridge absorber, which makes use of the Euler-Lagrange equations.

2.4 Optimisation of the Stockbridge Absorber

Now, the secondary system (Stockbridge absorber) is attached to a primary system (electrical transmission line) resulting in a compound system. In order to optimise the physical dimensions of the absorber, an objective function has to be proposed. Here, the objective function will be defined from the maximum absolute values of the principal coordinate functions of the compound system. Assuming that the primary system has a very low and almost constant hysteretic damping, the equations of motion for the primary system in the frequency domain are:

$$[-\Omega^2 \mathbf{M}_{pr} + \mathbf{K}_{pr}] \mathbf{q}_{pr}(\Omega) = \mathbf{f}(\Omega) \quad (32),$$

where \mathbf{M}_{pr} is the mass matrix of the primary system, \mathbf{K}_{pr} is the complex stiffness matrix of the primary system, $\mathbf{q}_{pr}(\Omega)$ is the displacement vector of generalized coordinates, and $\mathbf{f}(\Omega)$ is the force vector. Using the theory of the equivalent generalized quantities [20], the compound system can be modelled as:

$$[-\Omega^2 [\mathbf{M}_{pr} + \mathbf{M}_{eq}(\Omega)] + j\Omega \mathbf{C}_{eq}(\Omega) + \mathbf{K}_{pr}] \mathbf{q}_{pr}(\Omega) = \mathbf{f}(\Omega) \quad (33),$$

where $\mathbf{M}_{eq}(\Omega)$ is the equivalent mass matrix and $\mathbf{C}_{eq}(\Omega)$ is the equivalent damping matrix.

If p absorbers are attached to the primary system, at the generalized physical coordinates q_{k1} ,

q_{k2}, \dots, q_{kp} , the equivalent generalized mass and damping matrices are:

$$\mathbf{M}_{eq}(\Omega) = \begin{bmatrix} 0 & 0 & \dots & 0 & 0 \\ 0 & m_{eq}(\Omega)_{k1} & \dots & 0 & 0 \\ 0 & 0 & \ddots & 0 & 0 \\ 0 & 0 & \dots & m_{eq}(\Omega)_{kp} & 0 \\ 0 & 0 & \dots & 0 & 0 \end{bmatrix} \quad (34),$$

and

$$\mathbf{C}_{eq}(\Omega) = \begin{bmatrix} 0 & 0 & \dots & 0 & 0 \\ 0 & c_{eq}(\Omega)_{k1} & \dots & 0 & 0 \\ 0 & 0 & \ddots & 0 & 0 \\ 0 & 0 & \dots & c_{eq}(\Omega)_{kp} & 0 \\ 0 & 0 & \dots & 0 & 0 \end{bmatrix} \quad (35),$$

respectively.

Using the transformation:

$$\mathbf{q}_{pr}(\Omega) = \Phi_{pr} \hat{\mathbf{p}}_{pr}(\Omega) \quad (36),$$

where Φ_{pr} is the matrix of the eigenvectors associated with the eigenvalues of the primary system in the frequency band of interest, and $\hat{\mathbf{p}}_{pr}$ is the vector of the principal coordinates of the primary system, Eq. (33) can be written as:

$$[-\Omega^2 [\mathbf{I} + \mathbf{M}_A(\Omega)] + j\Omega \mathbf{C}_A(\Omega) + \Sigma_{pr}] \hat{\mathbf{p}}_{pr}(\Omega) = \mathbf{n}(\Omega) \quad (37),$$

where $\mathbf{M}_A(\Omega) = \Phi_{pr}^T \mathbf{M}_{eq}(\Omega) \Phi_{pr}$, $\mathbf{C}_A(\Omega) = \Phi_{pr}^T \mathbf{C}_{eq}(\Omega) \Phi_{pr}$, $\mathbf{n}(\Omega) = \Phi_{pr}^T \mathbf{f}(\Omega)$, and $\Sigma_{pr} = \Phi_{pr}^T \mathbf{K}_{pr} \Phi_{pr} = \text{tr}(\sigma_l)$ is a trace matrix of eigenvalues of the primary system. Consequently:

$$\hat{\mathbf{p}}_{pr}(\Omega) = [-\Omega^2 [\mathbf{I} + \mathbf{M}_A(\Omega)] + j\Omega \mathbf{C}_A(\Omega) + \Sigma_{pr}]^{-1} \mathbf{n}(\Omega) \quad (38),$$

and the receptance matrix can be calculated by:

$$\alpha(\Omega) = \Phi_{pr} [-\Omega^2 [\mathbf{I} + \mathbf{M}_A(\Omega)] + j\Omega \mathbf{C}_A(\Omega) + \Sigma_{pr}]^{-1} \Phi_{pr}^T \quad (39).$$

Then, in order to solve the optimisation problem it is possible to define an objective function \bar{f} as the modulus of a vector formed by the maximum absolute values of the generalized principal coordinates of the primary system [20]. This can be expressed by the equation:

$$\bar{f}(\mathbf{x}) = \left\| \max_{\Omega_1 \leq \Omega \leq \Omega_2} \hat{\mathbf{p}}_{pr}^i(\mathbf{x}, \Omega) \right\|^2 \quad (40),$$

where Ω_1 and Ω_2 are the lower and upper limits of the frequency band of interest, respectively, \mathbf{x} is a design vector of project variables to optimise, and $i=1, \dots, N$, where N is the total number of degrees of freedom of the primary system.

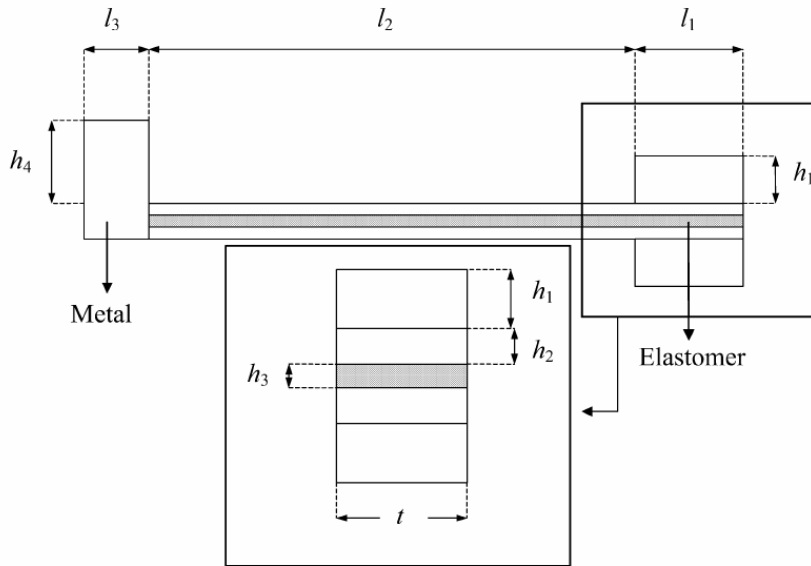


Fig. 6. Definitions of the physical dimensions to optimise for the Stockbridge absorber

The project variables to optimise are the physical dimensions of the absorber. Therefore, the design vector is defined as:

$$\mathbf{x} = [l_1, l_2, l_3, h_1, h_2, h_3, h_4, t]^T \quad (41),$$

where the elements of \mathbf{x} are the physical dimensions shown in Fig. 6. The constraint functions are defined for each element of \mathbf{x} as:

$$x_i^L \leq x_i \leq x_i^U \quad (42),$$

where x_i^L and x_i^U are the lower and upper limits for each element, respectively. For the force vector, a unit force at each excitation point of the primary system can be used, i.e., $\mathbf{f} = [1, 1, \dots, 1, 1]^T$.

A numerical example was performed for a real compound system. A total of four Stockbridge absorbers were attached to the primary system. In this example of a Stockbridge absorber the two sandwich beams are designed from two metal layers of steel 1020 and a viscoelastic core DYAD 601 (Soundcoat Co.). The finite element model of the absorber is shown in Fig. 5. The beams were divided into 114 elements. For the length and thickness of the core, 19 and 2 elements were used, respectively. This choice was found appropriate for both, representing efficiently the internal shear and determining the first four modes in the frequency band used. The mass at the centre was divided into 32 elements and the tuning masses were divided into 24 elements each. This choice is because the mechanical purposes of the masses do not require high discretization. All the elements are two-dimen-

sional lagrangian and quadratic solids, of nine nodes, and they are in a plane state of stress. This gives a total of 308 elements, 1319 nodes, and a total of $n=2638$ degrees of freedom. For simplicity, the temperature is assumed to be a constant.

The primary system considered was an ACRS partridge cable, 30.2 m long, clamped at both extremes and subjected to a tension of 9000 N. The cable was divided into 81 equally spaced elements. The central masses of the absorbers were attached at nodes 5, 35, 46, and 76 of the cable. These positions were selected in order to be far from the nodes of the cable, allowing the absorbers to control a large number of modes of the primary structure. Figure 7 shows the physical model of the compound system and its corresponding generalized equivalent quantities model.

Since the finite elements were in a plane state of stress, t does not change a lot during the optimisation process, so it was fixed at a value of 10 mm. The lower and upper limits for each x_i were chosen such that: 1) the weight and size of the absorbers should not be excessive, and 2) the thickness of the elastomer should be small in order to have shear deformation from the vibration of the sandwich beams. The frequency range used to optimise the Stockbridge absorber was 40 to 60 Hz. The temperature was fixed at 10°C. Because of its nature, the objective function has a large number of local minima so a genetic algorithm was used to perform the optimisation. The theory and applications of the genetic algorithms in optimisation problems

Table 1. Results of the optimisation of the physical dimensions for the Stockbridge absorbers

x_i	x_i^L mm	x_i^U mm	x_i optimised mm
l_1	0	200	10.321
l_2	0	1000	210.002
l_3	0	200	30.024
h_1	0	100	10.096
h_2	0	10	2.013
h_3	0	5	2.000
h_4	0	400	30.102
t	–	–	10.000

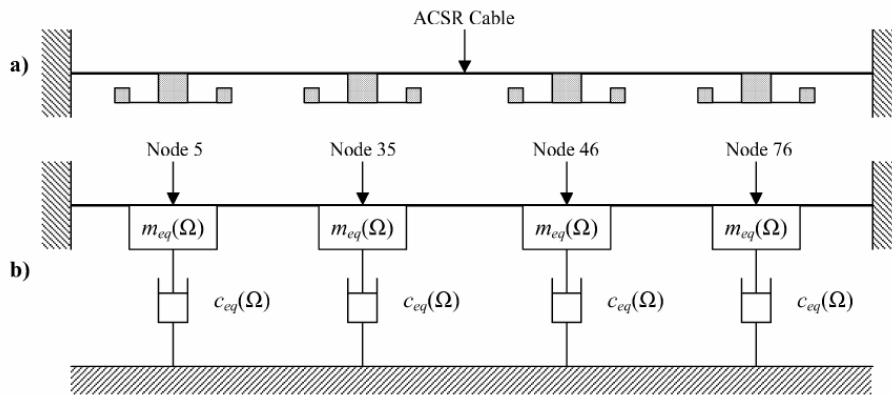


Fig. 7. Diagram of the compound system (cable plus Stockbridge absorbers): a) the physical model and b) its generalized equivalent quantities model

were explained in detail in the literature [21] to [23]. The numerical results of the optimisation process are presented in Table 1.

Figure 8 shows the results of the receptance at the mid point of the cable, when no absorber is attached, and when the absorbers are attached to the cable before and after the optimisation process. It can be seen that after their dimensions were optimised, the Stockbridge absorbers reduced the vibration level of the cable in a very effective way. Most of the peak values of the receptance frequency response were attenuated and for the peak value at around 60 Hz an attenuation of 30 dB was achieved after the optimisation.

3 CONCLUSIONS

The modelling of a metal-elastomer composite structure based on a finite element method has been presented. In addition, a methodology to reduce the computation time when dealing with frequency dependent matrices has proven to give good approximate results. It has to be noted that the precision of the approximation presented in Section 1

depends on the subspace. The factors that determine the behaviour of the algorithm are: a) the dimension \hat{n} of the subspace (a larger value of the dimension will produce a better approximation), and b) the variation of the complex shear modulus of the viscoelastic material with both frequency and temperature. It can be expected that in the transition zone the errors will be increased. As a result, the distance between the subspace generated by the truncated modal matrix $\hat{\Phi}_0$ and the space generated by the modal matrix Φ is increased. Obviously, this implies that the initial frequency Ω_0 plays an important role in the computations since the difference between $\mathbf{K}(\Omega_0, T)$ and $\mathbf{K}(\Omega, T)$ increases with the change of temperature. However, it can be concluded that the method used in this work seems to be quite efficient when compared to the subspace iteration method [8] and the Lanczos method [25], since these require the calculation of the inverse of the stiffness matrix for each iteration. In addition, a theory to determine the generalized equivalent quantities for a Stockbridge dynamic absorber has been presented. The use of these quantities does not add more degrees of freedom to the primary system and the

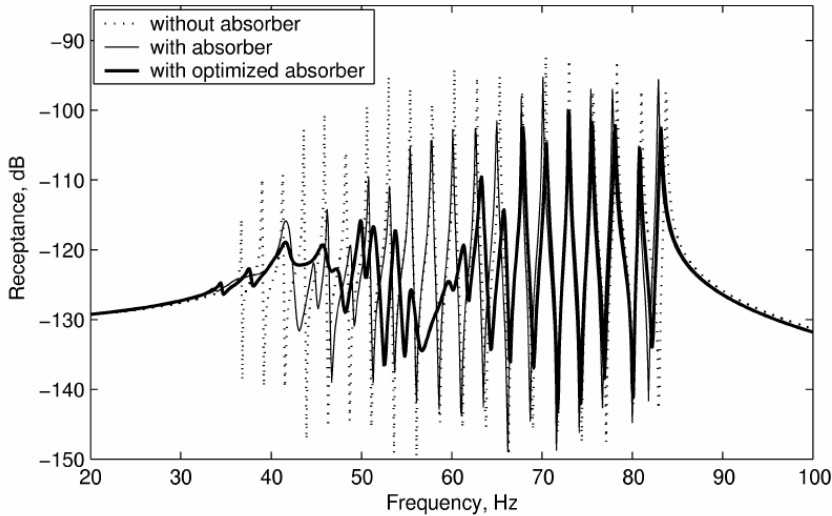


Fig. 8. Comparison of receptance frequency responses at the mid point of the primary system, with and without an optimised Stockbridge absorber

theory could be extended to other kinds of absorbers. Moreover, the use of generalized equivalent quantities allows one to define an objective function of the maximum absolute values of the principal coordinates of the primary structure. This objective function is independent of the geometry of the primary system and it is dependent on its modal parameters. The application of the method to Stockbridge absorbers used to suppress the aeolian vibrations of a real electrical transmission line shows that the

reduction in the response of up to eleven modes is achieved after the dimensions of the absorbers are optimised using a genetic algorithm. The optimisation process can be quite slow when compared to other techniques reported in the literature [18] and [19]; however, the results presented in this work seem to be encouraging. Further work will be conducted regarding the computational costs and detuning of the absorber due to the presence of temperature changes in the elastomer layer.

4 REFERENCES

- [1] Ross D., E.E. Ungar, E.M. Kerwin Jr. (1959) Damping of plate flexural vibrations by means of viscoelastic laminate structural damping, in *Structural Damping*, ASME, New York, pp. 49-88.
- [2] Soni, M.L. (1980) Finite element analysis of viscoelastically damped sandwich structures, in *Proc. of 51st Shock and Vibration Symposium*, San Diego, pp. 97-109.
- [3] Mignery, L. (1995) Vibration analysis of metal/polymer/metal components, in *Proc. of ASME Design Engineering Technical Conferences*, Vol. 3 (C), Boston, pp. 23-33.
- [4] Lumsdaine, A., R.A. Scott (1995) Shape optimisation of unconstrained beam and plate damping layers, in *Proc. of ASME Design Engineering Technical Conferences*, Vol. 3 (C), Boston, pp. 15-22.
- [5] Ungar, E.E. (1998) Vibration isolation and damping, Chapter 55 in *Handbook of Acoustics* (Edited by M.J. Crocker), John Wiley and Sons, New York.
- [6] Crandall, S.H. (1991) The hysteretic damping model in vibration theory. *Proc. of the Institute of Mechanical Engineers*, Part C, *Journal of Mechanical Engineering Science* 205(1), pp. 23-28.
- [7] Hughes, T.J.R. (2000) *The finite element method*, Dover, New York.
- [8] Bathe, K.J. (1995) *Finite elements procedures*, Prentice-Hall, New York.
- [9] Petyt, M. (1990) *Introduction to finite element vibration analysis*, Cambridge University Press, Cambridge.
- [10] Espindola, J.J., C.A. Bavastrri (1997) Reduction of vibration in complex structures with viscoelastic neutralizers - a generalized approach and a physical realization, in *Proc. of ASME Design Engineering Technical Conferences*, Sacramento (CD-Rom).

- [11] ASTM E 756-98 (1998) Standard test method for measuring vibration-damping properties of materials, *ASTM*, New York.
- [12] Vecchiarelli, J., I.G. Currie, D. G. Havard (2000) Computational analysis of aeolian conductor vibration with a Stockbridge-type damper. *J. of Fluids and Structures* 14(4), pp. 489-509.
- [13] Richardson, A.S. (1996) Performance requirements for vibration dampers. *Electric Power Systems Research* 36(1), pp. 21-28.
- [14] den Hartog, J.P. (1956) Mechanical vibrations, *McGraw-Hill*, New York, 1956.
- [15] Snowden, J.C. (1966) Vibration of cantilever beams to which dynamic absorbers are attached. *J. of the Acoust. Soc. Am.* 39(5), pp. 878-886.
- [16] Brennan, M.J. (1998) Control of flexural waves on a beam using a tunable vibration neutraliser. *J. Sound and Vib.* 222(3), pp. 389-407.
- [17] Kidner, M., M.J. Brennan (1999) Improving the performance of a vibration neutraliser by actively removing damping. *J. Sound and Vib.* 221(4), pp. 587-606.
- [18] Brennan, M.J., J. Dayou (2000) Global control of vibration using a tunable vibration neutralizer. *J. Sound and Vib.* 232(3), pp. 585-600.
- [19] Dayou, J., M.J. Brennan (2003) Experimental verification of the optimal tuning of a tunable vibration neutralizer for global vibration control. *Appl. Acoustics* 64(3), pp. 311-323.
- [20] Espindola, J.J., H.P. Silva (1992) Modal reduction of vibrations by dynamic neutralizers: a general approach, in *Proc. Tenth International Modal Analysis Conference*, San Diego, pp. 1367-1373.
- [21] Espindola, J.J., S.E. Floody (2001) Optimal design of Stockbridge dynamic vibration neutralizer viscoelastically modified applying the finite element method, in *Proc. 9th International Symposium on Dynamic Problems of Mechanics*, Florianópolis, pp. 507-513.
- [22] Rechenberg, I. (1993) Evolutionsstrategie: Optimierung technischer Systeme nach Prinzipien der biologischen Evolution (Evolution strategy: optimization of technical systems by means of principles of biological evolution), *Fromman-Holzboog*, Stuttgart.
- [23] Hung, S.L., H. Adeli (1994) A parallel genetic/neural network learning algorithm for MIMD shared memory machines. *IEEE Transactions Neural Networks* 5(6), pp. 900-909.
- [24] Espindola, J.J., C.A. Bavastri (1999) Optimum conceptual design of viscoelastic dynamic vibration neutralizer for low frequency complex structures, in *Proc. Int. Symposium on Dynamic Problems in Mechanic and Mechatronic*, Günzburg, pp. 251—259.
- [25] Lanczos, C. (1950) An iteration method for the solution of the eigenvalue problem of linear differential and integral operators. *Journal of Research of the National Bureau of Standards* 45(4), pp. 255-281.

Authors' Addresses: Prof. Dr. Sergio E. Floody
 Univ. Tecnológica de Chile
 Brown Norte 290
 Santiago, Chile
 s.floody@utecnologica.cl

Prof. Dr. Jorge P. Arenas
 Institute of Acoustics
 Univ. Austral de Chile
 PO Box 567, Valdivia, Chile
 jp Arenas@uach.cl

Prof. Dr. José J. de Espíndola
 Dept. Mechanical Engineering
 Univ. Federal de Santa Catarina
 Florianópolis, SC 80040-900, Brasil
 espindol@mbox1.ufsc.br

Prejeto:
 Received: 1.2.2006

Sprejeto:
 Accepted: 25.10.2006

Odrpoto za diskusijo: 1 leto
 Open for discussion: 1 year